International Journal of Engineering Trends and Technology (IJETT) – Volume 21 Number 1 – March 2015

Computational Drag Analysis of Passenger Car Using Splines and Spoiler

Vishal Shukla[1], Gaurav Saxena[2]

[1] *Research Scholar, Department of Automobile Engineering, RJIT BSF ACEDEMY Tekanpur*

[2] *Assistant Professor, Automobile Department , RJIT BSF ACEDEMY Tekanpur*

***Abstract*— The main aim of this paper is investigation of aerodynamics of passenger car, measuring drag coefficient. This work proposes an effective numerical model based on the Computational Fluid Dynamics (CFD) approach to obtain the flow structure around a passenger car with Splines and Rear Spoiler. The experimental work of the test vehicle and grid system is constructed by HYPERMESH. FLUENT which is the CFD solver & employed in the present work. In this study, numerical iterations are completed, then after aerodynamic data and detailed complicated flow structure are visualized.**

In the present work, model of generic passenger car has been developed in CATIA and generated the wind tunnel and applied the boundary conditions in HYPERMESH platform then after testing and simulation has been performed for the evaluation of drag coefficient for passenger car. In another case, the aerodynamics of the most suitable design of vortex generators is introduced and analyzed for the evaluation of drag coefficient for passenger car.

***Keywords*— Aerodynamic Drag , Coefficient of Drag, Coefficient of Lift, Wind tunnel simulation, Hypermesh FLUENT, Passenger car, CFD** .

I. INTRODUCTION

The rapidly increasing fuel prices and the regulation of green house gasses to control global warming give tremendous pressure on design engineers to enhance the current designs of the vehicle using the concepts of aerodynamics as to enhance the efficiency of vehicles [1]. Fuel consumption due to aerodynamic drag consumed more than half of the vehicle's energy. Thus, the drag reduction program is one of the most interesting approaches to cater this matter. Aerodynamic drag consists of two main components: skin friction drag and pressure drag. Pressure drag accounts for more than 80% of the total drag and it is highly dependent on vehicle geometry due to boundary layer separation from rear window surface and formation of wake region behind the vehicle. The location of separation determines the size of wake region and consequently, it determines the value of aerodynamic drag. According to Hucho [2], the aerodynamic drag of a road vehicle is responsible for a large part of the vehicle's fuel consumption and contributes up to 50% of the total vehicle fuel consumption at highway speeds. Reducing the aerodynamic drag offers an inexpensive solution to improve fuel efficiency and thus shape optimization for low drag become an essential part of the overall vehicle design process [3]. It has been found that 40% of the drag force is concentrated at the rear of the geometry [4]

In general, the design criteria of spoiler are only limited to considering the aerodynamics aspect due to the spoilers. Car drivers usually install spoilers that successfully reduce the drag and improve traction leading to better maneuver. However, the aero-dynamics performance corresponding to the spoiler has deteriorated severely. For this reason, this work has introduced the designers of spoiler a new direction, tool, and idea for spoiler design process. In the following sections, the methodology will be presented in detail.

II. VARIOUS STEPS OF WORK

In this work, first of all a generic model of the passenger car is prepared in the CATIA software and this generic model is import into the A HYPERMESH to do the simulation of the coefficient of drag and coefficient of lift in the wind tunnel which is generated in the design module HYPERMESH of the After this the meshing is generated on the surface of the passenger car.

Aerodynamic evaluation of air flow over an object can be performed using analytical method or CFD approach. On one hand, analytical method of solving air flow over an object can be done only for simple flows over simple geometries like laminar flow over a flat plate. If air flow gets complex as in flows over a bluff body, the flow becomes turbulent and it is impossible to solve Navier- Stokes and continuity equations analytically. On the other hand, obtaining direct numerical solution of Navier-stoke equation is not yet possible even with modern day computers. In order to come up with reasonable solution, a time averaged Navier-Stokes equation is being used (Reynolds Averaged Navier-Stokes Equations – RANS equations) together with turbulent models to resolve the issue involving Reynolds Stress resulting from the time averaging process.

In present work the k-e turbulence model with non-equilibrium wall function is selected to analyze the flow over the generic passenger car model. This k-e turbulence model is very robust, having reasonable computational turn around time, and widely used by the auto industry**.**

Steps of Analysis

- Select the models of vehicle upon which add on

devices are to be used.

- Formation of Base Line Model: Designing of model in CATIA with proper dimensions & parameters.
- Baseline passenger car CFD method and setup: Apply the boundary conditions.
- Simulation & Testing of base line passenger car for drag coefficient and lift coefficient.
- Simulation & Testing of passenger car with Splines and Spoiler for drag coefficient & lift coefficient
- Impact of add on devices on fuel economy of passenger car.

III. BASE LINE MODEL

The base line model of generic passenger car is designed in CATIA. Then after, this model has been analysed for drag coefficient and forces under the HYPERMESH (FULENT) module and values of drag coefficient, lift coefficient.

A. Summary

This report summarizes the results of an external aerodynamic CFD analysis performed by Altair's Virtual Wind Tunnel, leveraging AcuSolve's CFD technology.
The first section provides a brief overview of the run and its results.

Simulation type	"transient"
Element count	532321
CPU time	0.029 h
Inflow velocity	30 m/s
Drag coefficient, Cd	0.604
Lift coefficient, Cl	0.25

Table 1: Problem Information

B. Dimensions

This sections contains geometric dimensions related to the wind tunnel and the body.

Wind tunnel, bounding box	[0.000, 7.000], [-2.000, 2.000], [0.000, 3.000]
Body, bounding box	[1.661, 4.140], [-0.540, 0.540], [0.039, 1.224]
Wind tunnel dimension	7.000 m x 4.000 m x 3.000 m.
Body dimension	2.478 m x 1.080 m x 1.185 m.
Frontal ref. area, Aref	1.0363 m^2
Blockage ratio %	8.63583333333
Distance inflow – body	1.661 m

Table 2: Geometric Dimensions

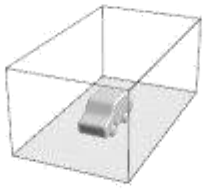

Figure 1: Virtual Wind Tunnel

C. Mesh

This section contains mesh statistics and screen shots of several cutting planes through the mesh.

Number. of nodes	99025
Number. of elements	532321
Number. of refinement zones	0

Table 3: Mesh statistics

Figure 2	Symmetry plane
Figure 3	Cross section

Table 4: Cutting planes through mesh

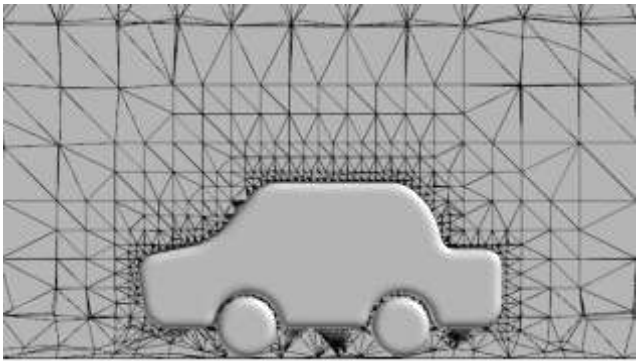

Figure 2: Mesh in Flow Direction

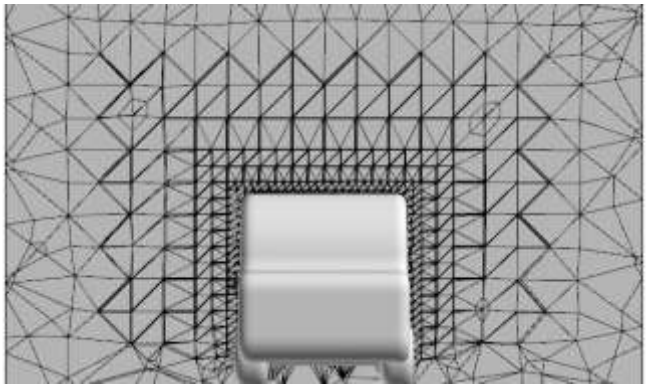

Figure 3: Mesh in Cross Direction

D. Boundary Conditions and Solution Strategy

In this section the boundary conditions and the setup for the CFD run are listed.

Inflow velocity	30 m/s
Outflow	Pressure outlet
Slip Walls	Top, right, left faces of wind tunnel
No-slip Walls	wind tunnel ground, body, wheels, heat-exchange

Table 5: Boundary conditions

Simulation type	"transient"
Number of time steps	5
Time increment	0.2
Physical time	1.000
Turbulence model	Detached Eddy Simulation
Moving ground	True
Rotating wheels	True

Table 6: Solution Strategy

E. Results

In this section the results of the CFD run are reported. Table 7 gives an overview of the different result types.

Table 8	Drag, lift and cross coefficient of individual parts and their totals
Table 9	Drag area of individual parts and their total
Figure 4	Drag, lift and cross coefficient history
Figure 5, 6, 7	Pressure contours on body, symmetry and cross section plane
Figure 8	Pressure coefficient on body surface
Figure 9, 10	Velocity contours on symmetry and horizontal cut plane
Figure 11, 12	Streamlines around body
Figure 13, 14, 15	Body Surface y+ contours

Table 7: Results

Surface	Drag Coefficient	Lift Coefficient	Cross Coefficient
Part1	0.60381	0.25075	0.00867
Total	0.603808284661	0.250752907872	0.00866803798449

Table 8: Coefficient

Surface	Drag Area
Part1	0.62573
Total	0.625726525395

Table 9: Drag Areas

To compute the above aerodynamic coefficients, the following equations are used

$$\text{Drag coefficient, } C_d = \frac{2\ F_x}{\text{rho}\ v^2\ A_{ref}}$$

$$\text{Lift coefficient, } C_l = \frac{2\ F_z}{\text{rho}\ v^2\ A_{ref}}$$

$$\text{Cross coefficient, } C_c = \frac{2\ F_y}{\text{rho}\ v^2\ A_{ref}}$$

Fx; Fy; andFz; forces are acting on the body in x, y and z directions, respectively

rho is density of air (1.225 kg/m^3)

v is free stream velocity

A_{ref} is frontal projected area of the object

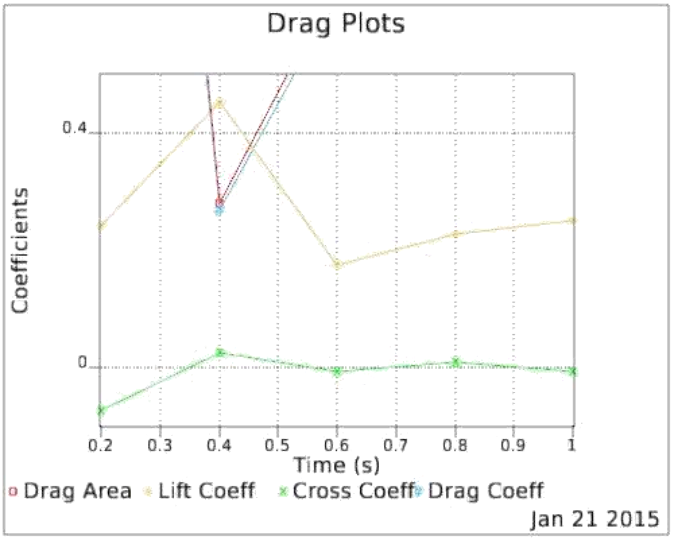

Figure 4: Coefficients

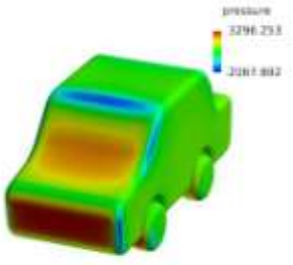

Figure 5: Body Surface Pressure Contours

Figure 6: Mid Plane Pressure Contours

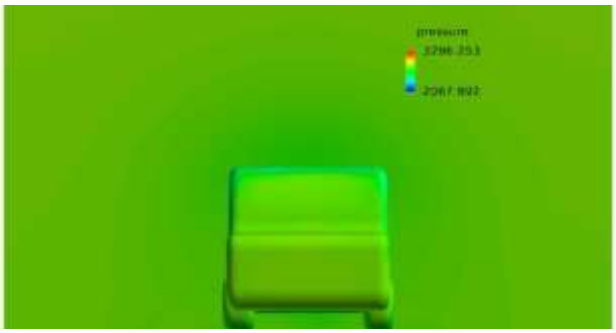

Figure 7: Cross Plane Pressure Contours

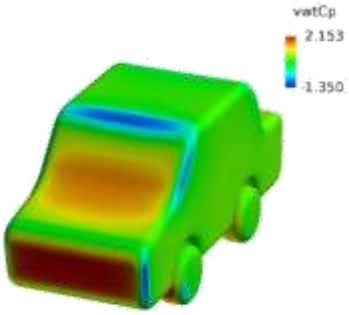

Figure 8: Body Surface Pressure Coefficient

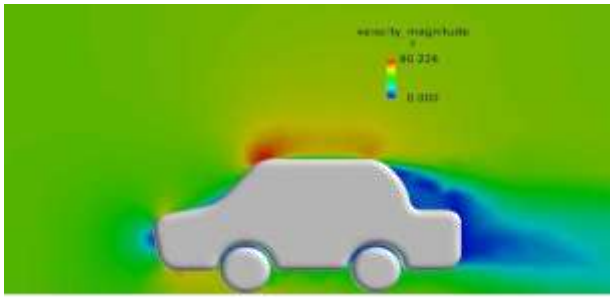

Figure 9: Mid Plane Velocity Contours

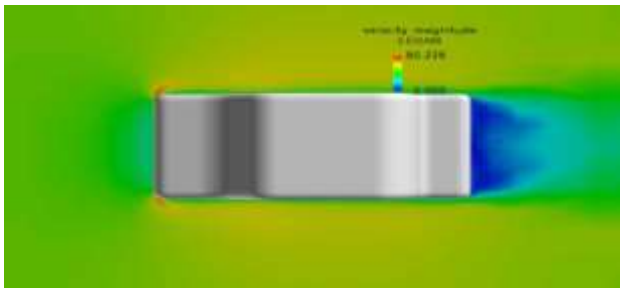

Figure 10: Cross Plane Velocity Contours

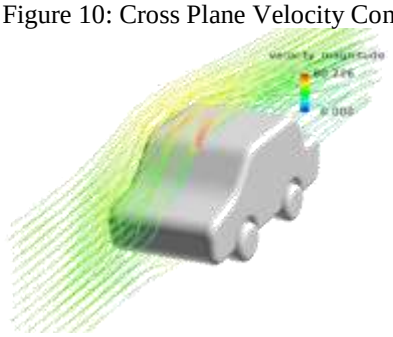

Figure 11: Stream lines

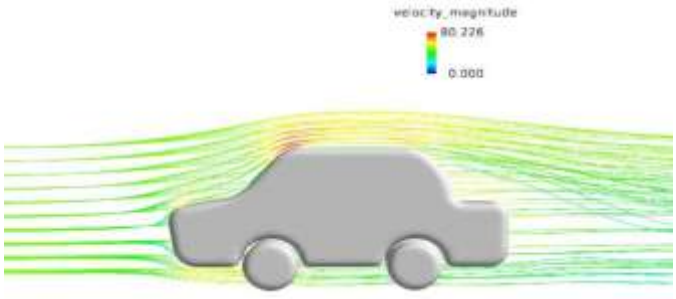

Figure 12: Stream lines Side View

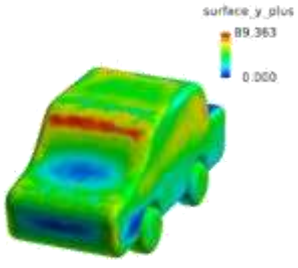

Figure 13: Body Surface y+ Front View

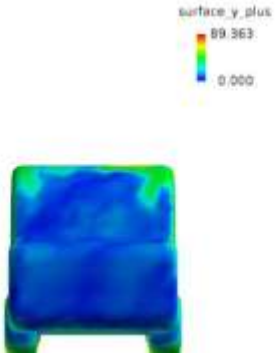

Figure 14: Body Surface y+ Rear View

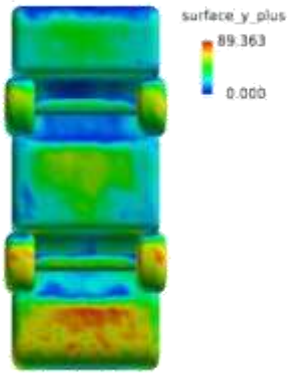

Figure 15: Body Surface y+ Bottom View

IV. PASSENGER CAR WITH SPLINES AND REAR SPOILER

The model of generic passenger car is designed in CATIA. Then after, this model has been analysed for drag coefficient and forces under the HYPERMESH (FULENT) module and values of drag coefficient, lift coefficient.

A. Summary

This report summarizes the results of an external aerodynamic CFD analysis performed by Altair's Virtual Wind Tunnel, leveraging AcuSolve's CFD technology.
The first section provides a brief overview of the run and its results.

Simulation type	"transient"
Element count	1054672
CPU time	0.050 h
Inflow velocity	30 m/s
Drag coefficient, Cd	0.511
Lift coefficient, Cl	0.003

Table 1: Problem Information

B. Dimensions

This sections contains geometric dimensions related to the wind tunnel and the body

Wind tunnel, bounding box	[0.000, 7.000], [-2.000, 2.000], [0.000, 2.000]
Body, bounding box	[1.897, 4.376], [-0.540, 0.540], [0.102, 1.298]
Wind tunnel dimension	7.000 m x 4.000 m x 2.000 m.
Body dimension	2.478 m x 1.080 m x 1.196 m.
Frontal ref. area, Aref	1.0462 m^2
Blockage ratio %	13.0775
Distance in inflow – body	1.897 m

Table 2: Geometric Dimensions

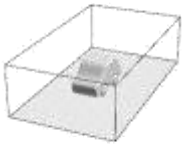

Figure 1: Virtual Wind Tunnel

C. Mesh

This section contains mesh statistics and screen shots of several cutting planes through the mesh.

Number. of nodes	190858
Number. of elements	1054672
Number. of refinement zones	0

Table 3: Mesh statistics

Figure 2	Symmetry plane
Figure 3	Cross section

Table 4: Cutting planes through mesh

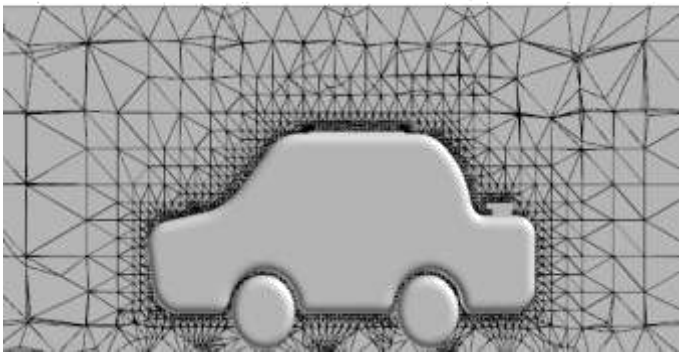

Figure 2: Mesh in Flow Direction

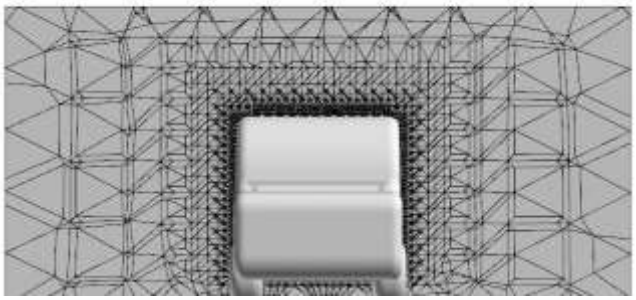

Figure 3: Mesh in Cross Direction

D. Boundary conditions and solution strategy

In this section the boundary conditions and the setup for the CFD run are listed.

In flow velocity	30 m/s
Outflow	Pressure outlet
Slip Walls	Top, right, left faces of wind tunnel
No-slip Walls	wind tunnel ground, body, wheels, heat-exchange

Table 5: Boundary conditions

Simulation type	"transient"
Number of time steps	4
Time increment	0.5
Physical time	2.000
Turbulence model	Detached Eddy Simulation
Moving ground	True
Rotating wheels	True

Table 6: Solution Strategy

E. Results

In this section the results of the CFD run are reported. Table 7 gives an overview of the different result types

Table 8	Drag, lift and cross coefficient of individual parts and their totals
Table 9	Drag area of individual parts and their total
Figure 4	Drag, lift and cross coefficient history
Figure 5, 6, 7	Pressure contours on body, symmetry and cross section plane
Figure 8	Pressure coefficient on body surface
Figure 9, 10	Velocity contours on symmetry and horizontal cut plane
Figure 11, 12	Streamlines around body
Figure 13, 14, 15	Body Surface y+ contours

Table 7: Results

Surface	Drag Coefficient	Lift Coefficient	Cross Coefficient
Part1	0.51125	0.22700	0.00328
Total	0.511250666091	0.227002058 39	0.003279146 36123

Table 8: Coefficients

Surface	Drag Area
Part1	0.53487
Total	0.534870446865

Table 9: Drag Areas

To compute the above aerodynamic coefficients, the following equations are used

$$\text{Drag coefficient, } C_d = \frac{2\ F_x}{\text{rho}\ v^2\ A_{ref}}$$

$$\text{Lift coefficient, } C_l = \frac{2\ F_z}{\text{rho}\ v^2\ A_{ref}}$$

$$\text{Cross coefficient, } Cc = \frac{2\ F_y}{\text{rho}\ v^2\ A_{ref}}$$

Fx; Fy; and Fz; forces are acting on the body in x, y and z directions, respectively

rho is density of air (1.225 kg/m3)

v is free stream velocity

Aref is frontal projected area of the object

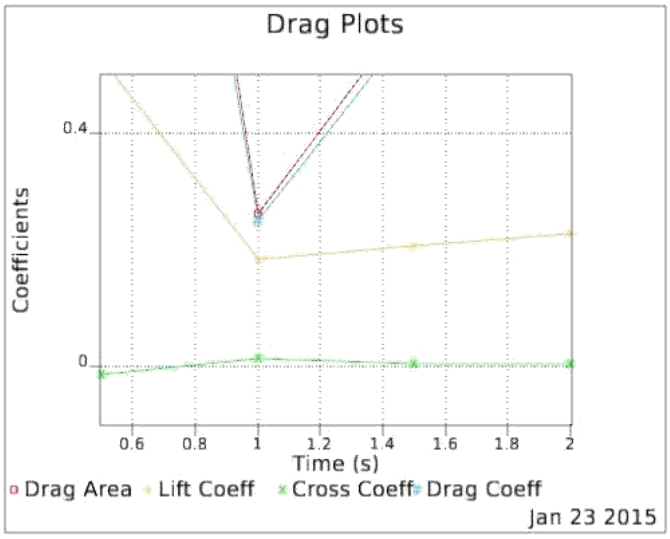

Figure 4: Coefficients

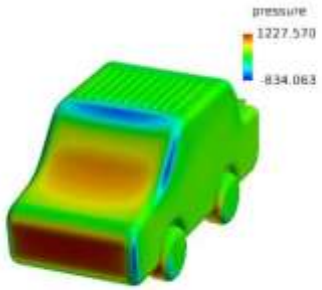

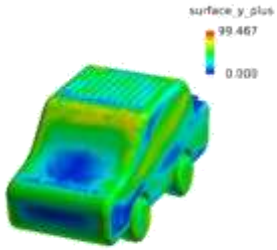

Figure 5: Body Surface Pressure Contours

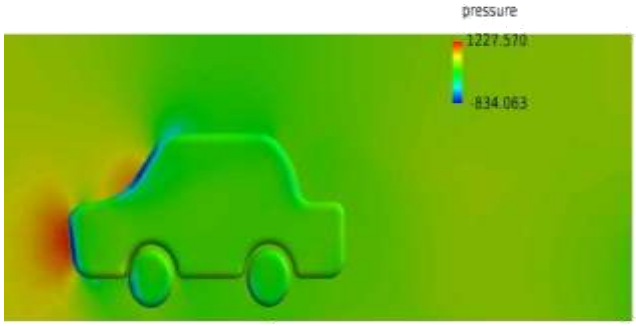

Figure 6: Mid Plane Pressure Contours

Figure 7: Cross Plane Pressure Contours

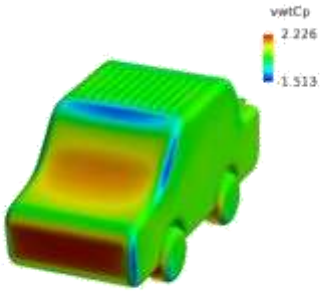

Figure 8: Body Surface Pressure Coefficient

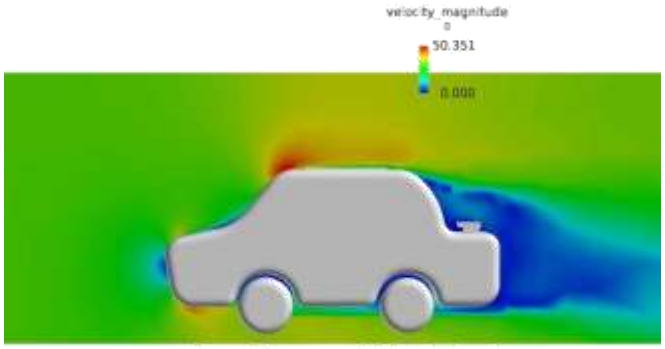

Figure 9: Mid Plane Velocity Contours

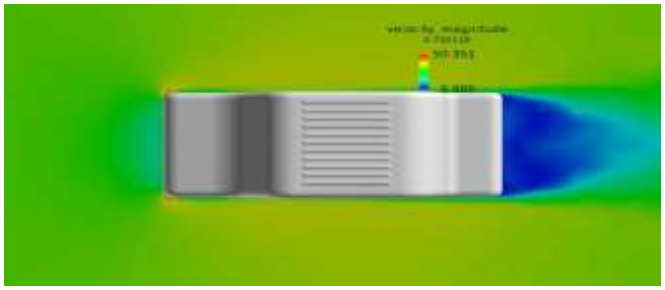

Figure 10: Cross Plane Velocity Contours

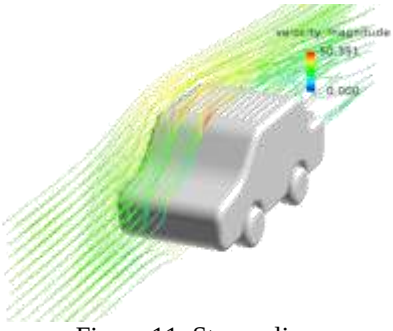

Figure 11: Stream lines

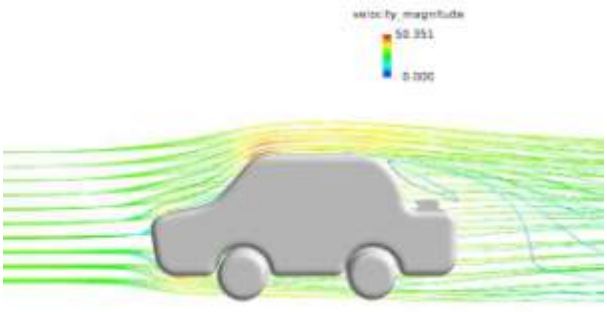

Figure 12: Stream lines Side View

Figure 13: Body Surface y+ Front View

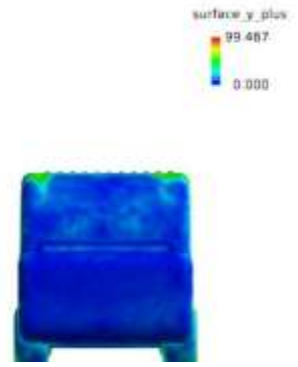

Figure 14: Body Surface y+ Rear View

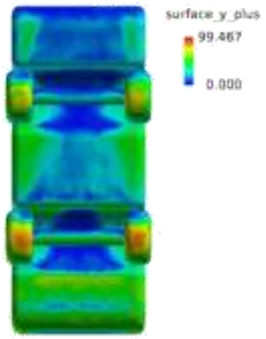

Figure 15: Body Surface y+ Bottom View

V. RESULT

In the case of SPLINES and the REAR SPOILER the coefficient of drag is 0.51 and the coefficient of lift is 0.22. The percentage reduction in drag coefficient in comparison of base line car is 15% and in coefficient of lift is 12%. Hence drag force & lift force on the passenger car is reduced as proportional to drag coefficient and lift coefficient respectively. The comparative results between the baseline car and car with spoiler are shown in table below:

Configuration	Drag coefficient	% reduction from base model	Lift coefficient	% reduction from base model
Base Model	0.60	0	0.25	0
Splines and Rear Spoiler	0.51	15%	0.22	12 %

Table 5.1 Drag and Lift coefficient of baseline Passenger car model with a model fitted with Splines and Rear Spoiler

VI. CONCLUSION

The effects of different aerodynamic add-on devices on flow and its structure over a generic passenger car may be analysed using CFD approach. The objective is to reduce aerodynamic drag acting on the vehicle and thus improve the fuel efficiency of passenger car. Hence, the drag force can be reduced by using add on devices on vehicle and fuel economy, stability of a passenger car can be improved.

REFERENCES

[1]Krishnani, P. N. (2009) CFD study of drag reduction of a generic sport utility vehicle, Master's Thesis, Mechanical Engineering Department, California State University, Sacramento.

[2] Hucho, W. H. and Sovran, G. (1993) Aerodynamics of road vehicles, Annual Review of Fluid Mechanics, Vol. 25(1), pp485-537 .

[3] Mayer, W., and Wickern, G. (2011) The new audi A6/A7 family-aerodynamic development of different body types on one platform, SAE International Journal of Passenger Cars-Mechanical Systems, Vol. 4(1), pp197-206.

[4] Chainani. A, and Perera. N, (2008) CFD Investigation of airflow

[5]Gilhaus, R. Hoffmann, Directional Stability, Aerodynamics of Road Vehicles, in: W.H. Hucho (Ed.), SAE International, Warrendale, PA, 1998.

[6]J.R. Callister, A.R. George, Wind Noise, Aerodynamics of Road Vehicles, in: W.H. Hucho (Ed.), SAE International, Warrendale, PA, 1998.

[7]F.R. Bailey, H.D. Simon, Future Directions in Computing and CFD, AIAA Paper 92-2734, 1992.

[8]H. Taeyoung, V. Sumantran, C. Harris, T. Kuzmanov, M. Huebler, T. Zak, Flow-field simulations of three simplified vehicle shapes and comparisons with experimental measurements, SAE Transactions 106 (1996) 820–835.

[9]B. Lokhande, S. Sovani, J. Xu, Computational Aero-acoustic Analysis of a Generic Side View Mirror, SAE 2003-01-1698, 2003.

[10] Kourta, A., and Leclerc, C. (2013) Characterization of synthetic jet actuation with application to Ahmed body wake, Sensors and Actuators A: Physical. 192, pp13-26.

[11] Park, H., Cho, J. H., Lee, J., Lee, D. H., and Kim, K. H. (2013) Aerodynamic drag reduction of Ahmed model using synthetic jet array, SAE International Journal of Passenger Cars-Mechanical Systems, Vol 6(1), pp1-6.

[12] Kang, S. O., Jun, S. O., Park, H. I., Song, K. S., Kee, J. D., Kim, K. H., and Lee, D. H. (2012) Actively translating a rear diffuser device for the aerodynamic drag reduction of a passenger car, International Journal of Automotive Technology, Vol.13(4), pp583-592.

[13] Bruneau, C. H., Creusé, E., Depeyras, D., Gilliéron, P., & Mortazavi, I. (2010) Coupling active and passive techniques to control the flow past the square back Ahmed body, Computers & Fluids, Vol.39(10), pp1875- 1892.

[14] Heinemann, T., Springer, M., Lienhart, H., Kniesburges, S., and Becker, S. (2012) Active flow control on a 1: 4 car model, In 16th Int Symp on Applications of Laser Techniques to Fluid Mechanics Lisbon, Portugal, 09-12 July. [15] Littlewood, R. P., and Passmore, M. A. (2012) Aerodynamic drag reduction of a simplified squareback vehicle using steady blowing, Experiments in fluids, Vol. 53(2), pp519-529.